

Planet-Mediated Precision-Reconstruction of the Evolution of the Cataclysmic Variable HU Aquarius

S. Portegies Zwart

Leiden Observatory, Leiden University, PO Box 9513, 2300 RA, Leiden, The Netherlands

ABSTRACT

Cataclysmic variables (CVs) are binaries in which a compact white dwarf accretes material from a low-mass companion star. The discovery of two planets in orbit around the CV HU Aquarii opens unusual opportunities for understanding the formation and evolution of this system. In particular the orbital parameters of the planets constrains the past and enables us to reconstruct the evolution of the system through the common-envelope phase. During this dramatic event the entire hydrogen envelope of the primary star is ejected, passing the two planets on the way. The observed eccentricities and orbital separations of the planets in HU Aqr enable us to limit the common-envelope parameter $\alpha\lambda = 0.45 \pm 0.17$ or $\gamma = 1.77 \pm 0.02$ and measure the rate at which the common envelope is ejected, which turns out to be copious. The mass in the common envelope is ejected from the binary system at a rate of $\dot{m} = 1.9 \pm 0.3 M_{\odot}/yr$. The reconstruction of the initial conditions for HU Aqr indicates that the primary star had a mass of $M_{\text{ZAMS}} = 1.6 \pm 0.2 M_{\odot}$ and a $m_{\text{ZAMS}} = 0.47 \pm 0.04 M_{\odot}$ companion in a $a = 25\text{--}160 R_{\odot}$ (best value $a = 97 R_{\odot}$) binary. The two planets were born with an orbital separation of $a_a = 541 \pm 44 R_{\odot}$ and $a_b = 750 \pm 72 R_{\odot}$ respectively. After the common envelope, the primary star turns into a $0.52 \pm 0.01 M_{\odot}$ helium white dwarf, which subsequently accreted $\sim 0.30 M_{\odot}$ from its Roche-lobe filling companion star, grinding it down to its current observed mass of $0.18 M_{\odot}$.

Key words: methods: numerical planets and satellites: dynamical evolution and stability planetstar interactions planets and satellites: formation stars: individual: HU Aquarius stars: binaries: evolution

1 INTRODUCTION

The cataclysmic variable HU Aqr currently consists of a $0.80 M_{\odot}$ white dwarf that accretes from a $0.18 M_{\odot}$ main-sequence companion star (Schwope et al. 2011). The transfer of mass in the tight $a = 0.82 R_{\odot}$ orbit is mediate by the emission of gravitational waves and the strong magnetic field of the accreting star (Verbunt & Zwaan 1981). Since its discovery (Schwope et al. 1993), irregularities of the observed-calculated variations have led to a range of explanations, including the presence of circum-binary planets (Schwarz et al. 2009; Horner et al. 2012b; Goździewski et al. 2012). Detailed timing analysis has eventually led to the conclusion that the CV is orbited by two planets (Hinse et al. 2012), a $5.7 M_{\text{Jup}}$ planet in a $\sim 1205 R_{\odot}$ orbit with an eccentricity of $e = 0.20$ and a somewhat more massive ($7.6 M_{\text{Jup}}$) planet in a wider $1785 R_{\odot}$ and eccentric $e = 0.38$ orbit (Horner et al. 2012b). Although, the two-planet configuration turned out to be dynamically unstable on a 1000–10,000 year time scale (Horner et al. 2012b, see also § 4), a small fraction of the numerical simulations exhibit long term dynamical stability (for model B2 in Wittenmyer et al. 2012, see Tab. 1 for the parameters).

It is peculiar to find a planet orbiting a binary, in particu-

lar around a CV. While planets may be a natural consequence of the formation of binaries (Pelupey & Portegies Zwart 2012), planetary systems orbiting CVs could also be quite common. In particular because of recently timing residual in NN Serpentis (Beuermann et al. 2010; Horner et al. 2012a), DP Leonis (Beuermann et al. 2011) and QS Virgo (Almeida & Jablonski 2011) were also interpreted is being caused by circum-CV planets.

Although the verdict on the planets around HU Aqr (and the other CVs) remains debated (Tom Marsh private communication, and Qian et al. 2010), we here demonstrate how a planet in orbit around a CV, and in particular two planets, can constrain the CV evolution and be used to reconstruct the history of the inner binary. We will use the planets to perform a precision reconstruction of the binary history, and for the remaining paper we assume the planets to be real.

Because of their catastrophic evolutionary history, CVs seem to be the last place to find planets. The original binary lost probably more than half its mass in the common-envelope phase, which causes the reduction of the binary separation by more than an order of magnitude. It is hard to imagine how a planet (let alone two) can survive such turbulent past, but it could be a rather natural con-

sequence of the evolution of CVs, and its survival offers unique diagnostics to constrain the origin and the evolution of the system.

2 THE EVOLUTION OF A CV WITH PLANETS

After the birth of the binary, the primary star evolved until it overflowed its Roche lobe, which initiated a common-envelope phase. The hydrogen envelope of the primary was ejected quite suddenly in this episode (Webbink 1984), and the white dwarf still bears the imprint of its progenitor: the mass and composition of the white dwarf limits the mass and evolutionary phase of its progenitor star at the moment of Roche-lobe overflow (RLOF). For an isolated binary the degeneracy between the donor mass at the moment of RLOF (M_{RLOF}), its radius R_{RLOF} and the mass of its core M_{core} cannot be broken.

The presence of the inner planet in orbit around HU Aqr (Hinse et al. 2012; Horner et al. 2012b; Goździewski et al. 2012) allows us to break this degeneracy and derive the rate of mass loss in the common-envelope phase. The outer planet allows us to validate this calculation and in addition to determine the conditions under which the CV was born. The requirement that the initial binary must have been dynamically stable further constrains the masses of the two stars and their orbital separation.

2.1 Pre common envelope evolution

During the CV phase little mass is lost from the binary system $M_{\text{cv}} \simeq \text{constant}$ (but see Schenker & King 2002), and the current total binary mass ($M_{\text{cv}} = 0.98 M_{\odot}$) was not affected by the past (and current) CV evolution (Ritter 2010). The observed white dwarf mass then provides an upper limit to the mass of the core of the primary star at the moment of Roche-lobe contact, and therefore also provides a minimum to the companion mass via $m_{\text{comp}} \geq M_{\text{cv}} - M_{\text{core}}$.

With the mass of the companion not being affected by the common envelope phase, we constrain the orbital parameters at the moment of RLOF by calculating stellar evolution tracks to measure the core mass M_{core} and the corresponding radius $R(M_{\text{core}})$ for stars with zero-age main-sequence mass M_{ZAMS} . In Fig. 1 we present the evolution of the radius of a $3 M_{\odot}$ star as a function of M_{core} , which is a measure of time.

We adopted the Henyey stellar evolution code MESA (Paxton et al. 2011) to calculate evolutionary track of stars from $M_{\text{ZAMS}} = 1$ to $8 M_{\odot}$ using AMUSE¹ (Portegies Zwart et al. 2009, 2012) to run MESA and determine the mass of the stellar core. The latter is measured by searching for the mass-shell in the stellar evolution code for which the relative Hydrogen fraction $< 1.0^{-9}$ (Tauris & Dewi 2001).

At the moment of RLOF the core mass is M_{core} and the stellar radius $R_{\text{RLOF}} \equiv R(M_{\text{core}})$. Via the relation for the Roche radius (Eggleton 1983), we can now calculate the orbital separation at the moment of RLOF a_{RLOF} as a function of M_{RLOF} . This separation is slightly larger than the initial (zero-age) binary separation a_{ZAMS} due to the mass lost by the primary star since its birth

$M_{\text{RLOF}} - M_{\text{ZAMS}}$. The long (main-sequence) time scale in which this mass is lost guarantees an adiabatic response to the orbital separation, i.e. $aM_{\text{tot}} = \text{constant}$.

For each M_{ZAMS} we now have a range of possible solutions for a_{RLOF} as a function of M_{core} and $m_{\text{comp}} = M_{\text{cv}} - M_{\text{core}}$. This reflects the assumption that the total mass ($m_{\text{comp}} + M_{\text{core}} = 0.98 M_{\odot}$) in the observed binary with mass M_{cv} is conserved throughout the evolution of the CV. In Fig. 1 we present the corresponding stellar radius R_{RLOF} and a_{RLOF} as a function of M_{core} for $M_{\text{ZAMS}} = 3 M_{\odot}$. This curve for a_{RLOF} is interrupted when RLOF would already have been initiated earlier for that particular orbital separation. We calculate this curve by first measuring the size of the donor for core mass M_{core} , and assuming that the primary fills its Roche-lobe we calculate the orbital separation at which this happens.

2.2 The common envelope evolution

During the common envelope phase the primary's mantle is blown away beyond the orbit of the planets. The latter responds to this by migrating from the orbits in which they were born (semi-major axis a_a and eccentricity e_a , the subscript 'a' indicates the inner planet, we adopt a 'b' to indicate the outer planet) to the currently observed orbits. Using first order analysis we recognize two regimes of mass loss: fast and slow. In the latter case the orbit expands adiabatically without affecting the eccentricity: The minimum possible expansion of the planet's orbit is achieved when the common envelope is lost adiabatically. Fast mass loss leads to an increase in the eccentricity as well and may even cause the planet to escape (Hills 1983; Pijloo et al. 2012).

A planet born at the shortest possible orbital separation to be dynamically stable will have $a_a \sim 3a_{\text{ZAMS}}$ (Mardling & Aarseth 2001), which is slightly smaller than the distance at which circum binary planets tend to form (Pelupey & Portegies Zwart 2012). In Fig. 1 we present a minimum to the semi-major axis for a planet that was born at $a_a = 3a_{\text{ZAMS}}$ and migrated by the adiabatic loss of the hydrogen envelope from the primary star in the common-envelope phase. The planet can have migrated to a wider orbit, but not to an orbit smaller than the solid black curve (indicated with $\min(a_a)$) in Fig. 1. For the $3 M_{\odot}$ star, presented in Fig. 1, RLOF can successfully result in the migration of the planet to the observed separation in HU Aqr for $M_{\text{core}} \lesssim 0.521 R_{\odot}$, which occurs for $a_{\text{ZAMS}} \lesssim 111 R_{\odot}$. A core mass $M_{\text{core}} > 0.521 R_{\odot}$ would, for a $3 M_{\odot}$ primary star, result in an orbital separation that exceeds that of the inner planet in HU Aqr; in this case the core mass of the primary star must have been smaller than $0.521 M_{\odot}$.

Another constraint on the initial binary orbit is provided by the requirement that the mass transfer in the post common-envelope binary should be stable when the companion starts to overfill its Roche lobe. To guarantee stable mass transfer we require that $m_{\text{comp}} \gtrsim M_{\text{core}}$. The thick part of the red curve in Fig. 1 indicates the valid range for the initial orbital separation and core-mass for which the observed planet can be explained; the thin parts indicate where these criteria fail.

We repeat the calculation presented in Fig. 1 for a range of masses from $M_{\text{ZAMS}} = 1 M_{\odot}$ to $8 M_{\odot}$ with steps of $0.02 M_{\odot}$, the results are presented as the shaded region in Fig. 2.

¹ The Astrophysics Multipurpose Software Environment, or AMUSE, is a component library with a homogeneous interface structure, and can be downloaded for free at amusecode.org. All the source codes and scripts for reproducing the calculations described in this paper are available via the AMUSE website.

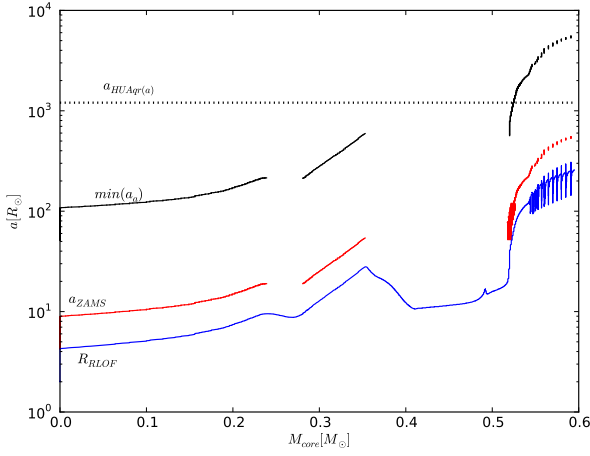


Figure 1. The orbital separation as a function of core mass for a primary star of $M_{\text{ZAMS}} = 3 M_{\odot}$. The thin blue curve (bottom) gives the stellar radius R_{RLOF} as a function of its core mass M_{core} , and the curve directly above that (red) gives the initial orbital separation a_{ZAMS} for which Roche-lobe overflow of that binary occurs. Here we adopted a companion mass of $m_{\text{comp}} = 0.98 M_{\odot} - M_{\text{core}}$ as in HU Aqr. The interruptions in the curves indicate the core masses for which Roche-lobe overflow cannot occur, because it would already have occurred in an earlier stage of the evolution, i.e., at a smaller core mass. The solid black curve (top) gives the minimal orbital separation of a planet born at $a_a = 3a_{\text{ZAMS}}$ for with the orbit was adiabatically expanded due to the mass loss in the common envelope $M_{\text{ZAMS}} - M_{\text{core}}$. The horizontal dotted curve gives the separation at which the inner planet around HU Aqr was observed. For viable solutions the solid black curve should remain below the horizontal dotted curve. The thick parts of the red curve indicate where the zero-age binary complies to the most favorable conditions for engaging RLOF, surviving the common-envelope and produce a planet that can migrate to at least the observed separation for the inner planet in HU Aqr.

3 EFFECT OF THE COMMON ENVELOPE PHASE ON THE PLANETARY SYSTEM

The response of the orbit of the planet to the mass loss depends on the total amount of mass lost in the common envelope and the rate at which it is lost. Numerical common-envelope studies indicate that for an in-spiraling binary $\dot{m} \simeq 2.0 M_{\odot}/\text{yr}$ (Ricker & Taam 2012). At this rate the entire envelope $M_{\text{RLOF}} - M_{\text{core}} \sim 0.46 - 5.8 M_{\odot}$ is expelled well within one orbital period of the inner planet, which leads to an impulsive response and the possible loss (for $M_{\text{RLOF}} - M_{\text{core}} \gtrsim 1.92 M_{\odot}$) of the planet. The fact that the HU Aqr is orbited by a planet indicates that at the distance of the planet $\dot{m}_a \ll (M_{\text{RLOF}} - M_{\text{core}})/P_{\text{planet}} \sim 1 M_{\odot}/\text{yr}$. The eccentricity of the inner planet in HU Aqr (see Tab. 1) can be used to further constrain the rate at which the common-envelope was lost from the planetary orbit. The higher eccentricity of the outer planet indicates a more impulsive response, which is a natural consequence of its wider orbits with the same \dot{m} . This regime between adiabatic and impulsive mass loss is hard to study analytically (Li 2008).

3.1 The response of the inner planet

We calculate the effect of the mass loss on the orbital parameters by numerically integrating the planet orbit. The calculations are started by selecting initial conditions for the zero-age binary HU

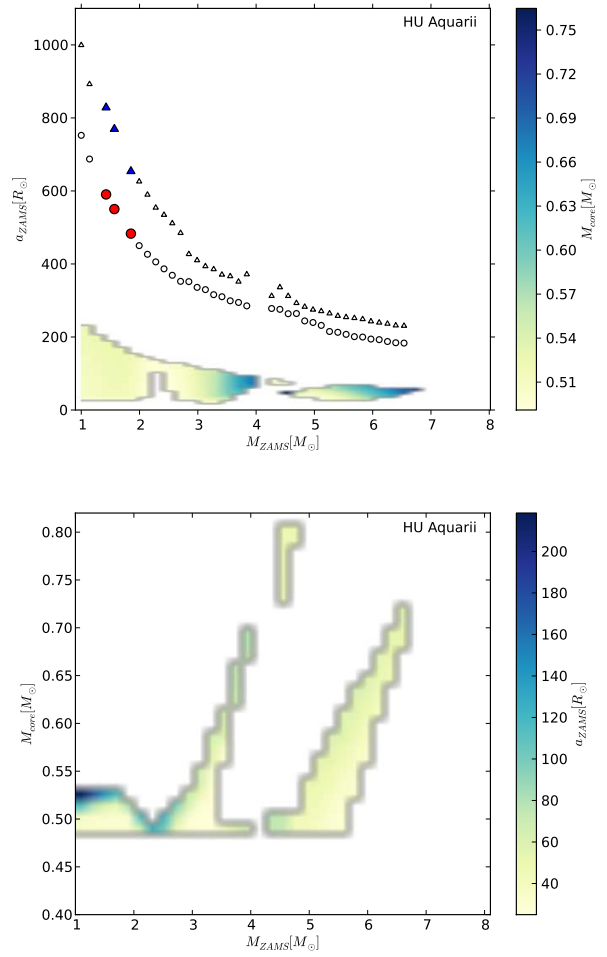


Figure 2. Distribution of initial conditions a_{ZAMS} and M_{ZAMS} , and the resulting core mass M_{core} (bottom panel) that successfully reproduce the CV HU Aqr. In the top panel we also present the results of our analysis for the two planets. The circles give the initial semi-major axis of the inner planet. The triangles give the initial semi-major axis for the outer planet. The symbols are colored (red for the inner planet and blue for the outer) if at least 10 out of 20 calculations for the orbital integration over 1 Myr turn out to be dynamically stable (see 4). With these initial conditions both planets migrate to within 1% of their observed orbital period with an eccentricity of $e_a = 0.20 \pm 0.01$ and $e_b = 0.33 \pm 0.03$ with $\dot{m}_a = 0.15 \pm 0.01 M_{\odot}/\text{yr}$.

Aqr- M_{ZAMS} , a_{ZAMS} and consequently M_{core} — from the available parameter space (shaded area) in Fig. 2, and integrate the equations of motion of the inner planet with time. Planets were assumed to be born in a circular orbit ($e_a = 0$) in the binary plane with semi-major axis a_a .

The equations of motions are integrated using the high-order symplectic integrator Huayno (Pelupessy et al. 2012) via the AMUSE framework. During the integration we adopt a constant mass-loss rate \dot{m} applied at every 1/100th of an orbit, and we continued the calculation until the entire envelope is lost (see § 2.2 and Fig. 2), at which time we measure the final semi-major axis and eccentricity of the planetary orbit. During the integration we allow the energy error to increase up to at most $\Delta E/E = 10^{-13}$.

By repeating this calculation while varying a_a and \dot{m}_a we iterate (by bisection) until the result is within 1% of the observed $a_{\text{HUAqr}}(a)$ and $e_{\text{HUAqr}}(a)$ of the inner planet observed in HU Aqr.

Table 1. Reconstructed and observationally constrained parameters for HU Aquarii. The parameters at zero-age (column 2 and 3) and directly after the common-envelope phase (columns 4 and 5) are derived by means of reconstructing the CV evolution. The best comparison is achieved for a mass loss rate in the common-envelope from the binary system of $\dot{m} = 1.9 \pm 0.3 \text{ M}_\odot/\text{yr}$ (or $\dot{m}_a = 0.15 \pm 0.01 \text{ M}_\odot/\text{yr}$ from the orbit of the first planet). Parameters that we were unable to constrain are printed in slanted font, observed parameters are from (Schwope et al. 2011; Hinse et al. 2012; Goździewski et al. 2012) and are printed in boldface.

parameter	Zero age		After CE		Today	
M/M_\odot	1.6 ± 0.2		0.52 ± 0.01		0.80 ± 0.04	
m/M_\odot	0.47 ± 0.04		0.47 ± 0.04		0.18 ± 0.06	
a/R_\odot	25–160		0.867–2.0		0.8	
e	0.0		0.0		0.0	
	planet a	planet b	planet a	planet b	planet a	planet b
a/R_\odot	541 ± 44	750 ± 72	1204 ± 12	1785 ± 18	1204	1785
m/M_{Jup}	5.7	7	5.7	7	5.7	7
e	0.0	0.0	0.20 ± 0.00	0.33 ± 0.03	0.20	0.38

The converged results of these simulations are presented in Fig. 2 (circles), and these represent the range of consistent values for the inner planet’s orbital separation $a_a = 183\text{--}752 \text{ R}_\odot$ as a function of $M_{\text{ZAMS}} = 1\text{--}8 \text{ M}_\odot$ and consistently reproduce the observed inner planet when adopting $\dot{m}_a = 0.124\text{--}0.267 \text{ M}_\odot/\text{yr}$. The highest value for \dot{m} is reached for $M_{\text{ZAMS}} = 2.85 \text{ M}_\odot$ at an initial orbital separation of $a_a = 427 \text{ R}_\odot$.

The orbital solution for the inner planet is insensitive to the semi-major axis of the zero-age binary a_{ZAMS} (for a fixed M_{ZAMS}), and each of these solutions were tested for dynamical stability, which turned out to be the case irrespective of the initial binary semi-major axis (as discussed in § 4).

3.2 The response of the outer planet

We now adopt the in § 3.1 measured value of \dot{m} to integrate the orbit of the outer planet. The effect of the mass outflow on the planet is proportional to the square of the density in the wind at the location of the planet (Kudritzki et al. 1992). We correct for this effect by reducing the mass loss rate in the common envelope that affects the outer planet by a factor $(a_b/a_a)^{3/2}$.

We use the same integrator and assumptions about the initial orbits as in § 3.1, but we adopt the value of \dot{m} from our reconstruction of the inner planet (see § 3.1). To reconstruct the initial orbital separation of the outer planet a_b , we vary this value (by bisection) until the final semi-major axis is within 1% of the observed orbit (see Tab. 1). The results are presented in Fig. 2 (triangles). The post common-envelope eccentricity of the outer planet then turn out to be $e_b = 0.38 \pm 0.07$.

4 STABILITY OF THE INITIAL SYSTEM

After having reconstructed the initial conditions of the binary system with its two planets we test its dynamical stability by integrating the entire system numerically for 1 Myr using the Huayno integrator (Pelupey et al. 2012). To test the stability we check the semi-major axis and eccentricity of both planets every 100 years. If any of these parameters change by a factor of two compared to the initial values or if the orbits cross we declare the system unstable, otherwise they are considered stable. The calculations are repeated with the 4th order Hermite predictor-corrector integrator ph4 (McMillan et al. 2012) within AMUSE to verify that the results are robust, which turned out to be the case. We then repeated this calculation ten times with random initial orbital phases and again

with a 1% Gaussian variation in the initial planetary semi-major axes. In Fig. 2 we present the resulting stable systems by coloring them red (circled) and blue (triangles), the unstable systems are represented by open symbols.

From the wide range of possible systems that can produce HU Aqr only a small range around $M_{\text{ZAMS}} = 1.6 \pm 0.2 \text{ M}_\odot$ turns out to be dynamically stable. The eccentricity of the outer orbit of the stable systems (which were stable for initial conditions within 1%) $e_b = 0.32 \pm 0.02$, which is somewhat smaller than the observed value for HU Aqr (Horner et al. 2012b, $e = 0.38 \pm 0.16$). These values are obtained with $\dot{m}_a = 0.15 \pm 0.01 \text{ M}_\odot/\text{yr}$. The small uncertainty in the derived value of \dot{m} is a direct consequence of its sensitivity to e_a and the small error on M_{ZAMS} from the requirement that the initial system is dynamically stable.

5 DISCUSSION AND CONCLUSIONS

We have adopted the suggestive results from the timing analysis of HU Aqr, that the CV is orbited by two planets, to reconstruct the evolution of this complex system. A word of caution is well placed in that these observations are not confirmed, and currently under debate (Tom Marsh private communication, and comments by the referee). However, the predictive power that such an observation would entail is interesting. The possibility to reconstruct the initial conditions of a CV by measuring the orbital parameters of two circum binary planets is a general result that can be applied to other binaries. For CVs in particular it enables us to constrain the value of fundamental parameters in the common-envelope evolution. This in itself makes it interesting to perform this theoretical exercise, irrespective of the uncertainty in the observations. On the other hand, the consistency between the observations and the theoretical analysis give some trust to the correctness of these observations.

The presence of one planet in an eccentric orbit around a CV allow us to calculate the rate at which the common-envelope was lost from the inner binary. A single planet provides insufficient information to derive the initial mass of the primary star, but allows us to derive the initial binary separation and planetary orbital separation to within about factor of 5, and the initial rate of mass loss from the common envelope to about a factor 2. A second planet can be used to further constrain these parameters to a few per cent accuracy and allows us to make a precision reconstruction of the evolution of the CV.

We have used the observed two planets in orbit around the CV HU Aqr to reconstruct its evolution, to derived its initial conditions

(primary mass, secondary mass, orbital separation, and the orbital separations of both planets) and to measure the rate of mass lost in the common-envelope parameters \dot{m} . By comparing the binary parameters at birth with those after the common-envelope phase we subsequently calculate the two parameters $\alpha\lambda$ and γ .

The measured rate of mass loss for HU Aqr of $\dot{m}_a = 0.15 \pm 0.01 M_\odot/\text{yr}$ from the inner planetary orbit, which from the binary system itself would entail a mass-loss rate of $\dot{m} = 1.9 \pm 0.3 M_\odot/\text{yr}$, when we adopt the initial binary to have a semi-major axis of $a_{\text{ZAMS}} \simeq 97 R_\odot$, which is bracketed by our derived range of $a_{\text{ZAMS}} = 25\text{--}160 R_\odot$. This is consistent with a mass-loss rate of $\dot{m} \simeq 2 M_\odot/\text{yr}$ from numerical common-envelope studies (Ricker & Taam 2012).

By adopting that the binary survives its common envelope at a separation between $\sim 0.87 R_\odot$ (at which separation the secondary star will just fill its Roche-lobe to the white dwarf) and $\sim 2 R_\odot$ (for gravitational wave radiation to drive the binary into Roche-lobe overflow within 10 Gyr), we derive the value of $\alpha\lambda = 0.2\text{--}2.0$ (for $a_{\text{ZAMS}} \simeq 97 R_\odot$ we arrive at $\alpha\lambda \simeq 0.45 \pm 0.17$). This value is a bit small compared to numerous earlier studies, which tend to suggest $\alpha\lambda \simeq 4.0$. The alternative γ -formalism for common-envelope ejection (Nelemans et al. 2000) gives a value of $\gamma = 1.63\text{--}1.80$ (for $a_{\text{ZAMS}} \simeq 97 R_\odot$ we arrive at $\gamma \simeq 1.77 \pm 0.02$), which is consistent with the determination of γ in 30 other CVs (Nelemans & Tout 2005).

The inner planet in HU Aqr formed at $(3.2\text{--}20.6)a_{\text{ZAMS}}$, with a best value of $5.3 \pm 0.45 a_{\text{ZAMS}}$, which is consistent with the planets found to orbit other binaries, like Kepler 16 (Doyle et al. 2011) and for Kepler 34 and 35 (Welsh et al. 2012), although these systems have lower primary mass and secondary mass stars.

It seems unlikely that more planets were formed inside the orbit of the inner most planet, even though currently there is sufficient parameter space for many more stable planets; in the zero-age binary there has not been much room for forming additional planets further in. It is however possible that additional planets formed further out and those, we predict, will have even higher eccentricity than those already found.

Acknowledgements It is a pleasure to thank Edward P.J. van den Heuvel, Tom Marsh, Inti Pelupessy, Nathan de Vries, Arjen van Elteren and the anonymous referee for comments on the manuscript and discussions. This work was supported by the Netherlands Research Council NWO (grants #612.071.305 [LGM], #639.073.803 [VICI] and #614.061.608 [AMUSE]) and by the Netherlands Research School for Astronomy (NOVA).

REFERENCES

- Almeida, L. A., Jablonski, F. 2011, in A. Sozzetti, M. G. Lattanzi, A. P. Boss (eds.), *IAU Symposium*, Vol. 276 of *IAU Symposium*, p. 495
- Beuermann, K., Buhmann, J., Diese, J., Dreizler, S., Hessman, F. V., et al. 2011, *A&A*, 526, A53
- Beuermann, K., Hessman, F. V., Dreizler, S., Marsh, T. R., Parsons, et al. 2010, *A&A*, 521, L60
- Doyle, L. R., Carter, J. A., Fabrycky, D. C., Slawson, R. W., Howell, et al. 2011, *Science*, 333, 1602
- Eggleton, P. P. 1983, *ApJ*, 268, 368
- Goździewski, K., Nasiroglu, I., Słowikowska, A., Beuermann, K., Kanbach, G., et al. A. 2012, *MNRAS*, 425, 930
- Hills, J. G. 1983, *ApJ*, 267, 322
- Hinse, T. C., Lee, J. W., Goździewski, K., Haghighipour, N., Lee, C.-U., Scullion, E. M. 2012, *MNRAS*, 420, 3609
- Horner, J., Wittenmyer, R. A., Hinse, T. C., Tinney, C. G. 2012a, *MNRAS*, 425, 749
- Horner, J., Wittenmyer, R. A., Marshall, J. P., Tinney, C. G., Butters, O. W. 2012b, *ArXiv* 1201.5730
- Kudritzki, R.-P., Hummer, D. G., Pauldrach, A. W. A., Puls, J., Najarro, F., Imhoff, J. 1992, *A&A*, 257, 655
- Li, L.-S. 2008, *Astronomy Reports*, 52, 806
- Mardling, R. A., Aarseth, S. J. 2001, *MNRAS*, 321, 398
- McMillan, S., Portegies Zwart, S., van Elteren, A., Whitehead, A. 2012, in R. Capuzzo-Dolcetta, M. Limongi, A. Tornambè (eds.), *Advances in Computational Astrophysics: Methods, Tools, and Outcome*, Vol. 453 of *Astronomical Society of the Pacific Conference Series*, 129
- Nelemans, G., Tout, C. A. 2005, *MNRAS*, 356, 753
- Nelemans, G., Verbunt, F., Yungelson, L. R., Portegies Zwart, S. F. 2000, *A&A*, 360, 1011
- Paxton, B., Bildsten, L., Dotter, A., Herwig, F., Lesaffre, P., Timmes, F. 2011, *ApJS*, 192, 3
- Pelupessy, F. I., Jänes, J., Portegies Zwart, S. 2012, *New Astronomy*, 17, 711
- Pelupessy, F. I., Portegies Zwart, S. 2012, submitted to *MNRAS* (ArXiv 1210.4678)
- Pijloo, J. T., Caputo, D. P., Portegies Zwart, S. F. 2012, *MNRAS*, 424, 2914
- Portegies Zwart, S., McMillan, S., Harfst, S., Groen, D., Fujii, M., et al. 2009, *New Astronomy*, 14, 369
- Portegies Zwart, S., McMillan, S., van Elteren, A., Pelupessy, I., de Vries, N. 2012, Accepted in *Computer Physics Communications*: ArXiv 1204.5522
- Qian, S.-B., Liao, W.-P., Zhu, L.-Y., Dai, Z.-B., Liu, L., et al. 2010, *MNRAS*, 401, L34
- Ricker, P. M., Taam, R. E. 2012, *ApJ*, 746, 74
- Ritter, H. 2010, *Mem. Soc. Astron. Italiana*, 81, 849
- Schenker, K., King, A. R. 2002, in B. T. Gänsicke, K. Beuermann, K. Reinsch (eds.), *The Physics of Cataclysmic Variables and Related Objects*, Vol. 261 of *Astronomical Society of the Pacific Conference Series*, 242
- Schwarz, R., Schwöpe, A. D., Vogel, J., Dhillon, V. S., Marsh, T. R., Copperwheat, C., Littlefair, S. P., Kanbach, G. 2009, *A&A*, 496, 833
- Schwöpe, A. D., Horne, K., Steeghs, D., Still, M. 2011, *A&A*, 531, A34
- Schwöpe, A. D., Thomas, H. C., Beuermann, K. 1993, *A&A*, 271, L25
- Tauris, T. M., Dewi, J. D. M. 2001, *A&A*, 369, 170
- Verbunt, F., Zwaan, C. 1981, *A&A*, 100, L7
- Webbink, R. F. 1984, *ApJ*, 277, 355
- Welsh, W. F., Orosz, J. A., Carter, J. A., Fabrycky, D. C., Ford, et al. 2012, *Nature*, 481, 475
- Wittenmyer, R. A., Horner, J., Marshall, J. P., Butters, O. W., Tinney, C. G. 2012, *MNRAS*, 419, 3258